



Lee, M.R. and Hodson, M.E. and Langworthy, G.N. (2008)  
*Crystallization of calcite from amorphous calcium carbonate:  
earthworms show the way.* Mineralogical Magazine, 72 (1). pp. 257-261.  
ISSN 0026-461X

<http://eprints.gla.ac.uk/24416/>

Deposited on: 06 January 2010

# Crystallization of calcite from amorphous calcium carbonate: earthworms show the way

M. R. LEE<sup>1,\*</sup>, M. E. HODSON<sup>2</sup> AND G. N. LANGWORTHY<sup>2,3</sup>

<sup>1</sup> Department of Geographical and Earth Sciences, Gregory Building, Lilybank Gardens, University of Glasgow, Glasgow, G12 8QQ, UK

<sup>2</sup> Department of Soil Science, School of Human and Environmental Science, University of Reading, RG6 6DW, UK

<sup>3</sup> ERM, Eaton House, Walbrook Court, North Hinksey Lane, Oxford OX2 0QS, UK

## Introduction

DARWIN (1881) was one of the first scientists to formally record that earthworms excrete calcium carbonate granules, with some up to 2 mm in diameter. However, since Darwin's studies they have received relatively little attention. The function of the granules remains a mystery, but may be related to regulation of Ca, CO<sub>2</sub>, pH or some other as yet undiscovered metabolic process (Robertson, 1936; Pearce, 1972). There has recently been an increase in research activity focussed on earthworm calcium carbonate granules driven by the work of Canti (Canti, 1998, 2007; Canti and Pearce, 2003) and largely relating to their potential use in archaeology. Canti determined granule production rates of 2.2 mg calcite day<sup>-1</sup> worm<sup>-1</sup> which translate into C processing rates of 60 kg C ha<sup>-1</sup> y<sup>-1</sup> via earthworm carbonate formation. These values indicate that granule production could play a small but significant role in the soil C cycle. Gago-Duport *et al.* (2008) have recently published the first detailed mineralogical study of the calcium carbonate granules and have traced their evolution from amorphous calcium carbonate (ACC) to calcite using scanning and transmission electron microscopy (SEM and TEM), Fourier transform infrared (FTIR) spectroscopy and X-ray diffraction (XRD). The aim of our complementary study has been to investigate the microstructures of the granules in order to determine the mechanisms by which they grow within the earthworm and subsequently crystallize to calcite.

## Methods

Clitellate *Lumbricus terrestris* (purchased from Blades Biological Ltd. Cowden, Edenbridge Kent, TN8 7DX, UK) were cultivated in soil collected from New Mayridge Farm (grid reference SU618703) which was sieved to <250 µm prior to use. Individual earthworms were cultivated in 5 cm diameter, 50 cm long polypropylene pipes each containing 415 g of moist soil and were fed 5 g of horse manure per week. After 28 days the soil was removed from the columns and wet-sieved to 250 µm. The >250 µm material was air-dried and stained with alizarin red to facilitate visual identification of the granules for hand-picking from the mixture. The majority of the granules were digested in 5% nitric acid to determine their trace element composition; we also analysed the alizarin red solution used for staining. The remaining granules were mounted in resin and polished for high-resolution imaging and chemical analysis. The granules in cross-section were imaged initially by optical cathodoluminescence (optical-CL), then coated with a thin layer of carbon and imaged using backscattered electrons (BSE) in a FEI Quanta 200F field-emission gun environmental scanning electron microscope (FEG-ESEM) operated at 20 kV. Following this initial characterization, high-resolution panchromatic CL images were acquired using the FEG-ESEM (i.e. SEM-CL images), which show net variations in emission intensity over the ultra-violet to infra-red wavelength range (Lee *et al.*, 2005). After removal of the carbon coating, charge contrast (CC) images were acquired from the granules with the FEG-ESEM operated in 'low vacuum' mode (chamber pressure ~60 Pa). These images are formed using secondary electrons and record variations in the degree of charge accumulation over the scanned area. The properties of the

\* E-mail: Martin.Lee@ges.gla.ac.uk  
DOI: 10.1180/minmag.2008.072.1.257

crystals that control the local degree of charge accumulation are poorly known, but probably relate to defect densities (Cuthbert and Buckman, 2005). Granule microstructures were characterized by electron backscatter diffraction (EBSD) employing an EDAX-TSL system attached to the FEG-ESEM, again in low vacuum mode. The EBSD generates backscatter Kikuchi patterns that can be indexed in order to determine the crystallographic orientation of the diffracting crystal and can also be used to distinguish crystalline from amorphous material by the presence and absence, respectively, of Kikuchi bands. The CL emission spectra spanning wavelengths 350–850 nm range were acquired using a Cameca SX100 electron probe operated at 20 kV and with a 2  $\mu\text{m}$  spot (Lee *et al.*, 2005).

## Results and discussion

The trace element composition of the granules is as follows. Because this is the first detailed compositional study of calcium carbonate granules to be published, every element present in our inductively coupled plasma optical emission spectroscopy (ICP-OES) multi-element standard has been included; values are the mean of three replicate batches of calcite granules with standard errors: 0.9 ( $\pm 0.1$ ) ppm Ag, 61 ( $\pm 8$ ) ppm Al, 47 ( $\pm 3$ ) ppm Ba, 3 ( $\pm 0.4$ ) ppm Cu, 153 ( $\pm 32$ ) ppm Fe, 7 ( $\pm 1$ ) ppm In, 352 ( $\pm 23$ ) ppm Mg, 174 ( $\pm 18$ ) ppm Mn, 55 ( $\pm 6$ ) ppm P, 5 ( $\pm 1$ ) ppm Pb, 345 ( $\pm 23$ ) ppm Sr and 10 ( $\pm 2$ ) ppm Zn. Elements that were analysed for but were below detection were (detection limits in brackets): B (3

ppm), Bi (11 ppm), Cd (0.1 ppm), Co (0.2 ppm), Cr (0.1 ppm), Ga (0.1 ppm), K (113 ppm), Li (0.5 ppm), Ni (0.1 ppm), Tl (0.1 ppm). Analysis of the alizarin red solution used to stain the granules gave the following concentrations, recalculated to the mass of the solid in the alizarin red solution: 160 ppm B, 6 ppm Co, 93822 ppm Fe, 23 ppm Ga, 195662 ppm K, 4 ppm Mg, 2 ppm Sr and 13 ppm Zn. On the basis of elements detected in the alizarin red solution, elements below detection limits in the calcite granules and calculated detection limits, the maximum concentrations of elements contributed to granules from the stain were: 8149 ppm Fe, 0.4 ppm Mg, 0.2 ppm Sr and 1 ppm Zn. Thus the majority, if not all the Fe detected in the granules is probably stain-derived but the Mg, Sr and Zn values most likely represent true concentrations in the granules.

The BSE images of polished cross-sections of the granules are shown in Fig. 1. Unlike those of Canti and Pearce (2003), the edges of these granules appear etched, which is due to slight dissolution during staining. The granules comprise an agglomeration of grains, predominantly calcium carbonate, and have complex internal structures; we identified two varieties, compact and concentrically laminated (Fig. 1*a*) and porous and structureless (Fig. 1*b*). All granules are circular to oval in cross section with aspect ratios of 1.0–1.7 (Fig. 1). They are composed predominantly of calcium carbonate but three of the 21 granules imaged had quartz cores 50–300  $\mu\text{m}$  in diameter (Fig. 1*a*). This percentage of quartz cores (14%) is consistent with all the granules having quartz cores, however

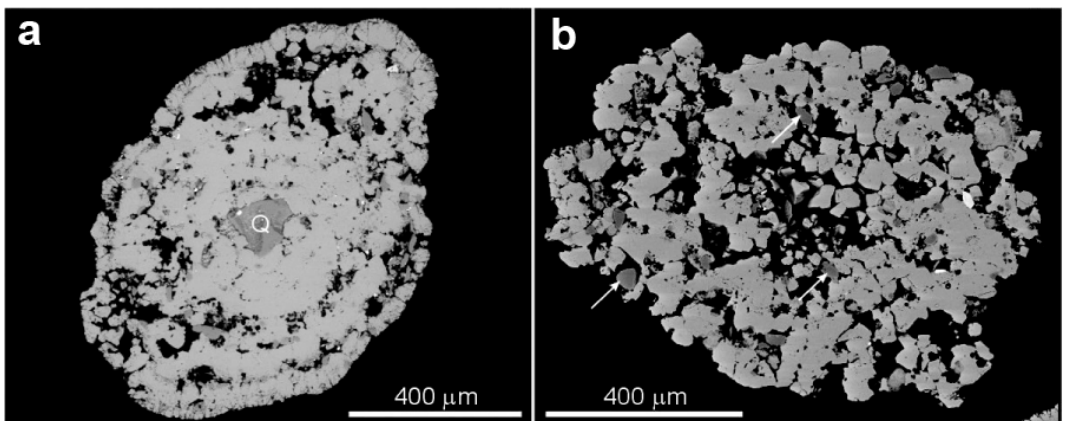


FIG. 1. BSE images of granules. (a) A compact granule with a quartz (Q) core and concentric internal structure; and (b) a porous and structureless granule containing numerous small quartz inclusions (arrowed).

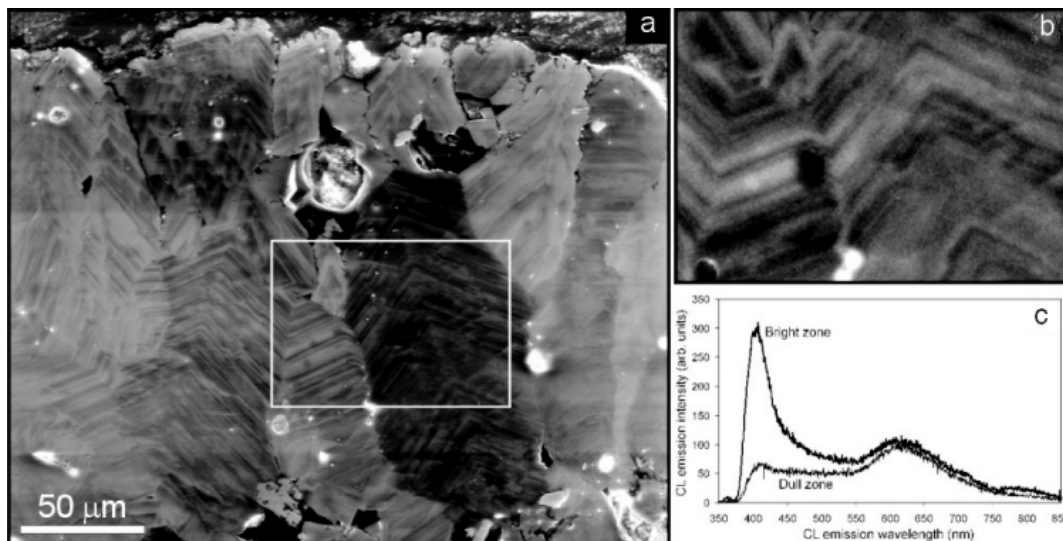


FIG. 2. (a) CC image of calcite close to a granule edge showing pervasive and very fine-scale zoning. (b) SEM-CL image of the boxed area in (a). Note the close correspondence in zoning patterns revealed by the two imaging techniques. (c) CL emission spectra from two wide zones identified by SEM-CL, one bright and one dull. These spectra indicate that the contrast in the SEM-CL image is due to variations in intensity of the  $\sim 400$  nm emission band whereas the  $\sim 600$  nm orange band shows little intensity variation.

they were only observed in granules cross-sectioned close to their centre. Quartz cores to earthworm calcium carbonate granules have not been reported previously and are likely to be of significance in their formation.

The EBSD mapping indicates that granules can contain both calcite and amorphous calcium carbonate (ACC). The calcite is most abundant and crystals are euhedral and interlocking. Granule calcite is a homogeneous orange in optical-CL, whereas higher resolution CC and SEM-CL imaging reveals intricate and fine-scale zoning (zone widths of  $\sim 200$ – $2000$  nm) in all crystals (Fig. 2*a,b*). The CL spectroscopy shows that the calcite has two luminescence emission peaks, at  $\sim 400$  nm (ultra-violet to blue) and  $\sim 600$  nm (orange) (Fig. 2*c*). The longer wavelength peak is indicative of  $\text{Mn}^{2+}$  activation whereas the ultra-violet to blue peak is the 'intrinsic' luminescence of calcite and likely to be activated by defects, possibly including those associated with  $\text{Fe}^{2+}$  substitution (Lee *et al.*, 2005). The zoning recorded by SEM-CL corresponds closely with variations in intensity of the  $\sim 400$  nm peak. The pattern of zoning recorded by SEM-CL is comparable to that in CC images (Fig. 2*a,b*), which is consistent with contrast in the CC images

also being determined by intracrystalline differences in defect density. The boundaries between zones are oriented parallel to calcite crystal terminations and traces of their  $\{10\text{--}14\}$  planes, thus demonstrating that they represent the former position of crystal faces. The EBSD mapping shows that granule calcite crystals, which tend to be elongate, are oriented with their long axes normal to the quartz core and granule edge (Fig. 3*a*). Calcite crystals also show a weak preferred orientation, with poles to  $\{0001\}$  planes lying at a low angle to the granule margin (Fig. 3*b*).

The ACC can be identified readily within the granules by its 'stromatolitic' appearance in BSE images (Fig. 4*a*) and the absence of diffraction bands in Kikuchi patterns (Fig. 4*b,c*). The ACC bodies are  $\sim 30$ – $300$  μm in size, usually enclosed by calcite, and comprise up to 20% of any one granule. The interface between calcite and ACC is sharp but irregular and the calcite cross-cuts the radial and concentric internal structure of the ACC. In contrast to Gago-Duport *et al.* (2008), we detected no aragonite or vaterite within the granules using EBSD.

Our observations suggest that the calcium carbonate spherulites previously observed to

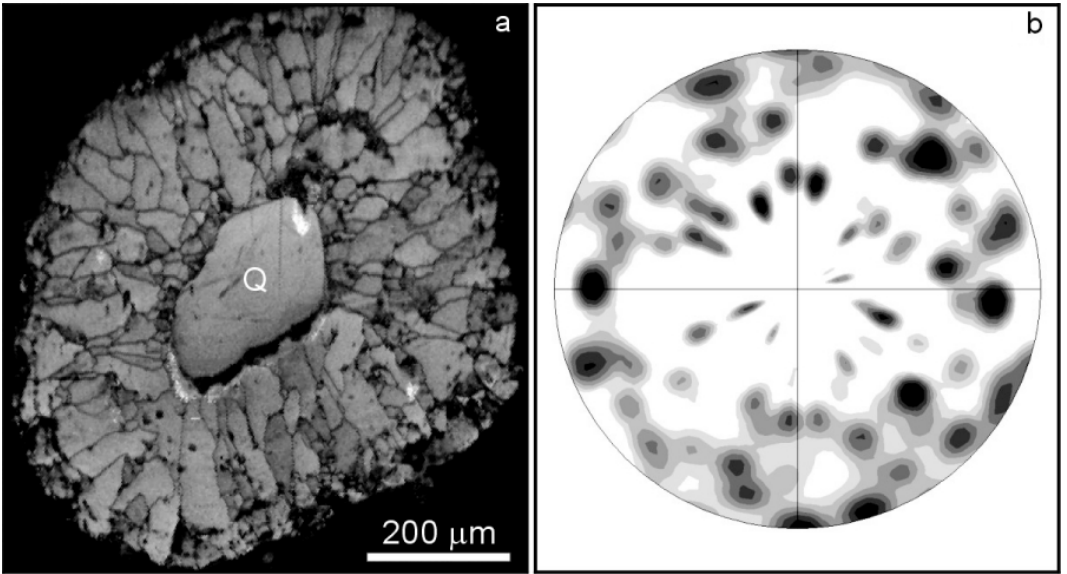


FIG. 3. Results of EBSD mapping of a granule. (a) Image quality map showing a large quartz core (Q) away from which radiate elongate calcite crystals. (b) Contoured  $\{0001\}$  equal angle pole figure of calcite crystals in (a) showing that the majority of crystals are oriented with  $\{0001\}$  at a low angle to the granule margin (i.e. close to the equator of the figure).

form in the earthworm calciferous gland (Morgan, 1981; Gago-Duport *et al.*, 2008) produce granules by adhering to large soil particles. The presence

of small quartz and feldspar inclusions within granules indicates that they grew gradually and by accretion of ACC spherulites in an environment

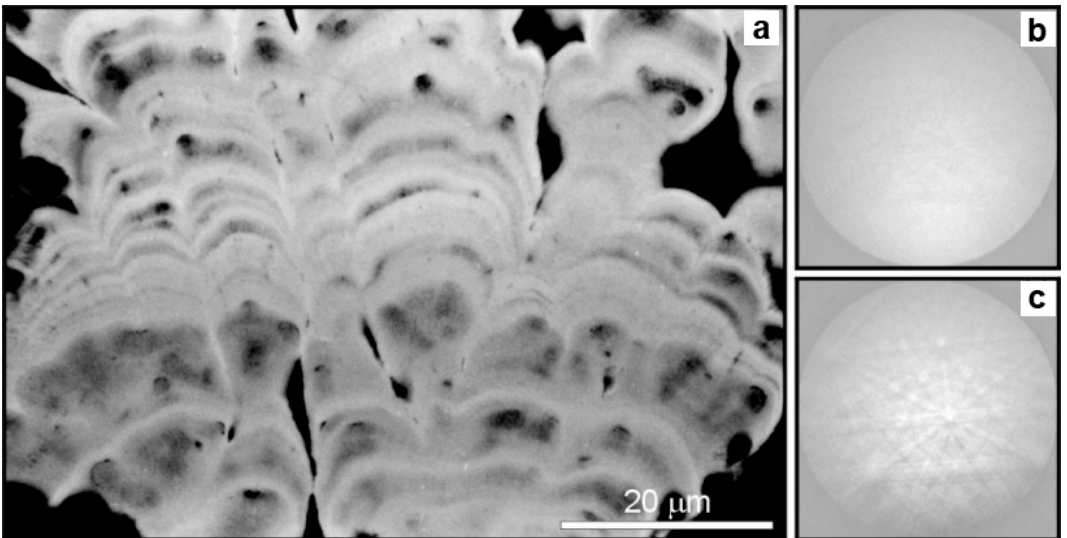


FIG. 4. (a) BSE image of an inclusion of ACC within a calcite granule displaying the very fine-scale 'stromatolitic' internal structure. (b) Backscatter Kikuchi pattern of the ACC illustrating its amorphous nature by lack of diffraction bands. (c) Backscatter Kikuchi pattern of granule calcite showing well-defined diffraction bands indicative of crystallinity.

that also contained ingested soil. In agreement with the findings of Gago-Duport *et al.* (2008), our results suggest that following accretion, the ACC crystallized to calcite, although we found no evidence for a vaterite precursor. The pattern of zoning in calcite indicates that crystallization took place by dissolution-reprecipitation as fluid films on calcite crystal faces migrated through the ACC and the fabric within granules revealed by EBSD indicates that crystals grew approximately radially outwards from the quartz nuclei. The calcite zoning has probably developed in response to regular fluctuations in trace-element concentrations of the fluids due to cyclical incorporation, depletion and replacement of solutes. We conclude that earthworm granules provide an unprecedented opportunity for detailed study of the processes and products of crystallization of ACC, which have important implications for understanding biomineralization throughout the animal kingdom.

### Acknowledgements

This work was supported by NERC grant NE/F009623/1 and a NERC studentship awarded to Graham Langworthy by the University of Reading Soils and Environmental Pollution Masters programme. We thank Sir William Benyon for permission to collect soil on the Englefield Estate and Mr John Jacks for making the calcite resin blocks.

### References

- Canti, M.G. (1998) Origin of calcium carbonate granules found in buried soils and Quaternary deposits. *Boreas*, **27**, 275–288.

- Canti, M.G. (2007) Deposition and taphonomy of earthworm granules in relation to their interpretative potential in Quaternary stratigraphy. *Journal of Quaternary Science*, **22**, 111–118.
- Canti, M.G. and Pearce, T.G. (2003) Morphology and dynamics of calcium carbonate granules produced by different earthworm species. *Pedobiologia*, **47**, 511–521.
- Cuthbert, S.J. and Buckman, J.O. (2005) Charge contrast imaging of fine-scale microstructure and compositional variation in garnet using the environmental scanning electron microscope. *American Mineralogist*, **90**, 701–707.
- Darwin, C. (1881) *The Formation of Vegetable Mould, Through the Action of Worms, with Observations on their Habits*. John Murray, London.
- Gago-Duport, L., Briones, M.J.I., Rodriguez, J.B. and Covelo, B. (2008) Amorphous calcium carbonate biomineralisation in the earthworm's calciferous gland: pathways to the formation of crystalline phases. *Journal of Structural Biology*, (in press).
- Lee, M.R., Martin, R.W., Trager-Cowan, C. and Edwards, P. R. (2005) Imaging of cathodoluminescence zoning in calcite by scanning electron microscopy and hyperspectral mapping. *Journal of Sedimentary Research*, **75**, 313–322.
- Morgan, A.J. (1981) A morphological and electron microprobe study of the inorganic composition of the mineralized secretory products of the calciferous gland and chloragogenous tissue of the earthworm *Lumbricus terrestris*. *L. Cell and Tissue Research*, **220**, 829–844.
- Pearce, T.G. (1972) The calcium relations of selected Lumbricidae. *Journal of Animal Ecology*, **41**, 167–188.
- Robertson, J.D. (1936) The function of the calciferous glands of earthworms. *Journal of Experimental Biology*, **13**, 279–297.